

Effect of heat treatment on mechanical dissipation in Ta₂O₅ coatings

I W Martin¹, R Bassiri¹, R Nawrodt^{1,2}, M M Fejer³,
A Gretarsson⁴, E Gustafson⁵, G Harry⁶, J Hough¹,
I MacLaren¹, S Penn⁷, S Reid¹, R Route³, S Rowan¹,
C Schwarz², P Seidel², J Scott¹ and A L Woodcraft^{8,9}

¹ SUPA†, Department of Physics and Astronomy, University of Glasgow, Glasgow, G12 8QQ, Scotland.

²Institute of Solid State Physics, University of Jena, Helmholtzweg 5, D-07743 Jena, Germany.

³ Edward L Ginzton Laboratory, Stanford University, Stanford, CA 94305-4088, USA.

⁴ Embry-Riddle Aeronautical University, Prescott, AZ 86301, USA.

⁵ LIGO Laboratory, California Institute of Technology 18-34, Pasadena, CA 91125, USA.

⁶ LIGO Laboratory, Massachusetts Institute of Technology, Cambridge, MA 02139, USA.

⁷ Department of Physics, Hobart and William Smith Colleges, Geneva, NY 14456, USA.

⁸ SUPA†, Institute for Astronomy, University of Edinburgh, Blackford Hill, Edinburgh EH9 3HJ, Scotland.

⁹ UK Astronomy Technology Centre, Blackford Hill, Edinburgh EH9 3HJ, Scotland.

E-mail: i.martin@physics.gla.ac.uk

Abstract.

Thermal noise arising from mechanical dissipation in dielectric reflective coatings is expected to critically limit the sensitivity of precision measurement systems such as high-resolution optical spectroscopy, optical frequency standards and future generations of interferometric gravitational wave detectors. We present measurements of the effect of post-deposition heat treatment on the temperature dependence of the mechanical dissipation in ion-beam sputtered tantalum pentoxide between 11 K and 300 K. We find the temperature dependence of the dissipation is strongly dependent on the temperature at which the heat treatment was carried out, and we have identified three dissipation peaks occurring at different heat treatment temperatures. At temperatures below 200 K, the magnitude of the loss was found to increase with higher heat treatment temperatures, indicating that heat treatment is a significant factor in determining the level of coating thermal noise.

PACS numbers: 05.40.Jc, 61.43.Er, 68.60.Bs, 04.80.Nn, 95.55.Ym, 42.60.Da

† Scottish Universities Physics Alliance

1. Introduction

Several long baseline gravitational wave detectors have been constructed and used in searches for gravitational radiation from astrophysical sources [1, 2, 3, 4]. These detectors use interferometric sensing to search for displacements, induced by gravitational waves, of test masses which are suspended as pendulums at the ends of perpendicular arms up to 4 km in length. The test masses are coated to form mirrors which are highly reflective at 1064 nm. The thermal displacement noise associated with the test mass mirrors is a significant limit to the sensitivity of these detectors [5, 6, 7]. The magnitude of the thermal noise is directly related to the mechanical dissipation of the materials used to construct the mirrors. In particular, the mechanical dissipation of the amorphous dielectric mirror coatings has been identified as an important noise source which is likely to limit the sensitivity of the generation of detectors currently being constructed, such as Advanced LIGO [8] and Advanced Virgo [9], in their most sensitive frequency band [10, 11, 12, 13]. Coating thermal noise is also expected to significantly limit the performance of highly frequency-stabilized lasers for use in high resolution optical spectroscopy [14], optical frequency standards [15, 16] and fundamental quantum measurements [17].

The mirror coatings used in current gravitational wave detectors are formed from alternating layers of silica (SiO₂) and tantalum pentoxide (Ta₂O₅) deposited by ion-beam sputtering. Research has shown that the mechanical dissipation of these multi-layer coatings is dominated by the dissipation of the Ta₂O₅ layers [18, 19, 20] and that the total dissipation of a multi-layer coating can be reduced by up to $\sim 40\%$ by doping the Ta₂O₅ with titania (TiO₂) [21]. However, neither the process responsible for mechanical dissipation in Ta₂O₅ nor the mechanism by which TiO₂ doping reduces the dissipation is as yet understood.

In a recent paper we reported data showing a low temperature dissipation peak in a Ta₂O₅ coating doped with TiO₂ and heat treated at 600 °C [22]. There is evidence that this peak arises from a thermally activated dissipation mechanism, possibly related to the reorientation of Ta-O bonds within a double well potential, similar to the mechanism believed to occur in fused silica [23, 24, 25]. Further work has suggested that the effect of the TiO₂ doping is to increase the activation energy of the dissipation process [26], thereby reducing the mechanical loss of the material. A barrier height distribution function analysis revealed that the effect of TiO₂ doping was to shift the distribution of potential barriers to a higher energy and to broaden the peak in the distribution. Heat treatment is another possible method of altering the distribution of potential barrier heights. Ion-beam sputtered coatings are often heat treated after deposition to reduce the stress in the film and to reduce the optical absorption [27]. Several studies have shown that post-deposition heat treatment of ion-beam sputtered amorphous oxide layers can increase the thickness of the film, with a corresponding reduction in density [27, 28, 29, 30]. Furthermore it is known heat treatment can significantly reduce the mechanical loss of bulk fused silica [31]. This is believed to be a result of a reduction of

internal stresses in the silica, possibly altering the distribution of the potential barrier heights [32]. Thus investigating the effects of heat treatment on the mechanical loss of Ta_2O_5 is of particular interest for understanding, and perhaps reducing, the mechanical dissipation. In addition to providing insights into the mechanisms of energy dissipation in Ta_2O_5 , measurements of the temperature dependence of the coating dissipation are critical for the design of future gravitational wave detectors such as ET [33] and LCGT [34] which may use cryogenic cooling to reduce thermal noise.

2. Sample preparation and experimental technique

The Ta_2O_5 coatings were deposited onto rectangular silicon cantilever substrates. These substrates consist of a 0.5-mm-thick clamping block and a thinner flexing portion of length 34-mm and thickness $50\text{ }\mu\text{m}$, as shown in Figure 1. The sample geometry was designed to reduce frictional energy losses into the clamp used to support the cantilever during mechanical loss measurements [35, 36]. A thermal oxide layer of approximately 30 nm thickness was grown on the cantilevers prior to coating to ensure proper adhesion of the Ta_2O_5 . A Ta_2O_5 film (0.49 ± 0.1) μm in thickness was deposited on one face of the flexing part of each cantilever by ion-beam sputtering using argon as the sputtering ion. Four fused silica disks, 25.4 mm in diameter, were coated in the same coating run to serve as witness samples for microscopic analysis of the coating structure. A coated cantilever, a nominally identical uncoated cantilever and a coated silica disk were heat treated in air at each of the following temperatures: 300, 400, 600 and 800 °C. The samples were heated to the desired temperature at 2 °C per minute and held at this temperature for 24 hours after which they were allowed to cool naturally. The coating and heat treatment process was carried out by CSIRO†. Ion-beam sputtered Ta_2O_5 films

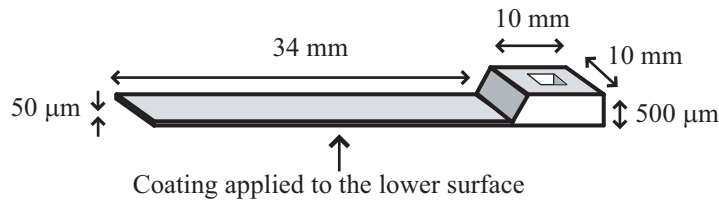


Figure 1. A schematic diagram of one of the silicon cantilever samples used for the coating loss measurements. The cantilever length is parallel to the $\langle 110 \rangle$ crystal axis.

have been observed to crystallize when heated to approximately 600 to 700 °C [37], to the detriment of their optical properties. The highest heat treatment temperature of 800 °C was chosen to allow study of the mechanical loss on either side of this transition region.

The mechanical dissipation factors of several resonant modes of each coated cantilever and the associated uncoated control cantilever were measured between 11

† Industrial Physics Division, Commonwealth Scientific and Industrial Research Organisation, West Lindfield, NSW, Australia

and 300 K in a cryostat using a ring-down technique, in which a resonant mode of the sample of angular frequency ω_0 was excited to an amplitude A_0 and the vibration allowed to decay freely. The time dependence of the amplitude ring-down $A(t)$ is given by:

$$A(t) = A_0 e^{-\phi(\omega_0)\omega_0 t/2}, \quad (1)$$

where $\phi(\omega_0)$ is the mechanical dissipation factor. The cantilever was mounted in a stainless steel clamp within the vacuum chamber of the cryostat and the bending modes excited by an electrostatic actuator located a few mm below the cantilever. The frequency of the n^{th} bending mode can be calculated as follows [38]:

$$\omega_n = \frac{\alpha_n^2 t}{4\pi\sqrt{3}L^2} \left(\frac{Y}{\rho}\right)^{1/2} \quad (2)$$

where ρ is the density, Y the Young's modulus, t the thickness and L the length of the cantilever. α_n is a numerical factor which takes the values 1.875, 4.694, 7.855 and 10.996 for $n = 1$ to 4 respectively. For $n \geq 5$, α_n can be approximated as $\alpha_n \simeq (2n - 1)\pi/2$. The vibration amplitude was measured by means of a laser beam reflected from the cantilever surface and directed onto a photodiode sensor outside the cryostat. The sensor consisted of a rectangular photodiode masked so that a thin triangular strip of the surface was exposed. Vibrations of the cantilever resulted in motion of the reflected laser beam along the triangular sensor, producing a signal proportional to the vibration amplitude. This sensor arrangement was found to be more practical than a quadrant photodiode due to the large amplitude of motion of the laser spot.

Several measurement cycles, in each of which the sample temperature was increased incrementally from 11 to 300 K, were carried out. Repeated ring-down measurements at each temperature generally showed a variation in loss factor of less than 5 % for each mode. The variation in the loss factor between the various temperature cycles was typically less than 10%. The temperature of the cantilever was measured using a silicon-diode sensor (Lakeshore DT-670 A) mounted within the clamp immediately below the fixed end of the cantilever.

3. Results

Figure 2 shows, as an example, the loss factors measured for the coated and uncoated cantilevers heat treated at 300 °C. The increase in loss due to the presence of the Ta_2O_5 film can be clearly observed throughout the temperature range studied. Of particular note is the peak in the loss of the coated cantilever at approximately 35 K - this will be discussed in more detail in the following section. The dissipation of the uncoated cantilever also exhibits a peak at between 25 to 30 K. A similar peak was observed for all of the uncoated samples studied. Peaks have been observed at similar temperatures in silica films grown on silicon by wet thermal oxidation [39], and it seems likely therefore that these peaks are due to the thermal oxide layer grown on all of the cantilevers.

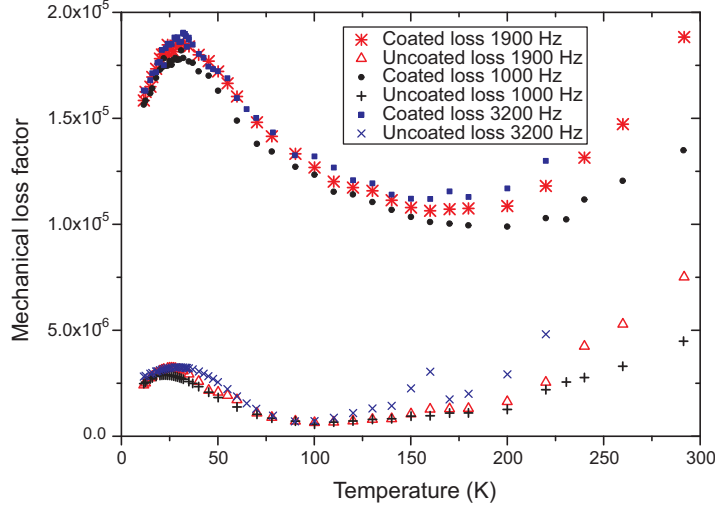


Figure 2. Measured mechanical loss for a cantilever coated with Ta_2O_5 and an uncoated control cantilever heat treated at $300^\circ C$

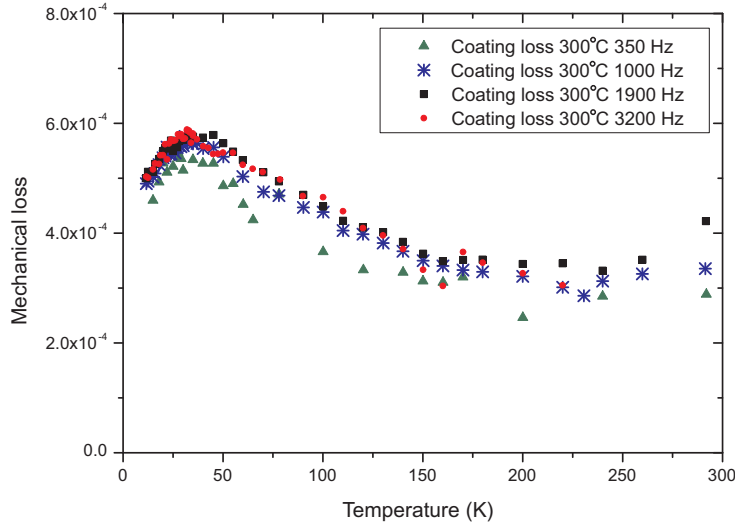


Figure 3. Mechanical loss of the Ta_2O_5 coating heat treated at $300^\circ C$ calculated from the measured data in Figure 2

The mechanical loss of the Ta_2O_5 film was calculated from the difference in the loss factors of the coated and uncoated cantilevers using the following equation [40]:

$$\phi(\omega_0)_{\text{coating}} = \frac{Y_s t_s}{3Y_c t_c} (\phi(\omega_0)_{\text{coated}} - \phi(\omega_0)_{\text{substrate}}), \quad (3)$$

where ω_0 is the angular frequency of the mode, $\phi(\omega_0)_{\text{coated}}$ is the loss factor of the coated cantilever, $\phi(\omega_0)_{\text{substrate}}$ is the loss factor of the cantilever prior to coating, t_s and Y_s are the thickness and Young's modulus of the substrate respectively and t_c and Y_c are respectively the thickness and Young's modulus of the coating. The Young's moduli of silicon and Ta_2O_5 were taken to be 166 GPa [41] and (140 ± 15) GPa [42] respectively. Assuming that the temperature dependence of the Young's modulus of Ta_2O_5 is typical

of other amorphous oxides [43], then its effect on the calculation over the temperature range studied here is negligible.

Figure 3 shows the calculated mechanical dissipation of the Ta_2O_5 film heat treated at 300°C, obtained from the data in Figure 2 using Equation 3. The same procedure was followed to find the loss of the coatings which had been heat treated at 400, 600 and 800°C. Data was obtained at several mode frequencies for each sample, and Figures 4 to 6 show comparisons of the loss of the series of coatings at 1000 Hz, 1900 Hz, 3000 Hz and 350 Hz respectively.

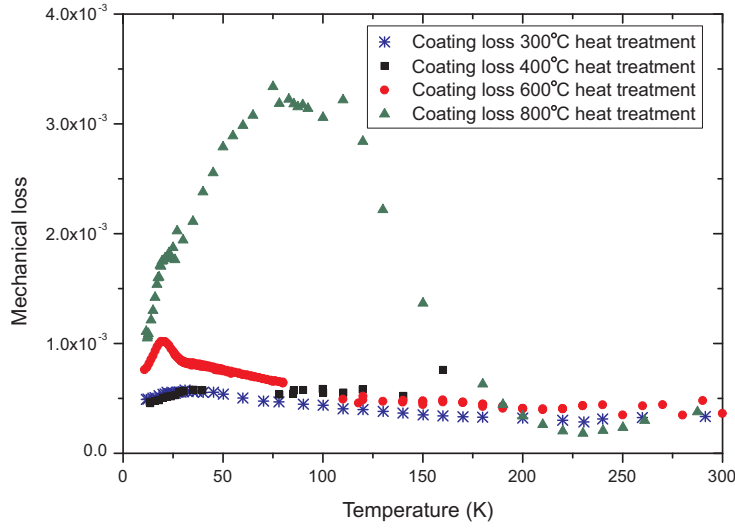


Figure 4. The calculated mechanical loss factors of the various Ta_2O_5 coatings at approximately 1000 Hz

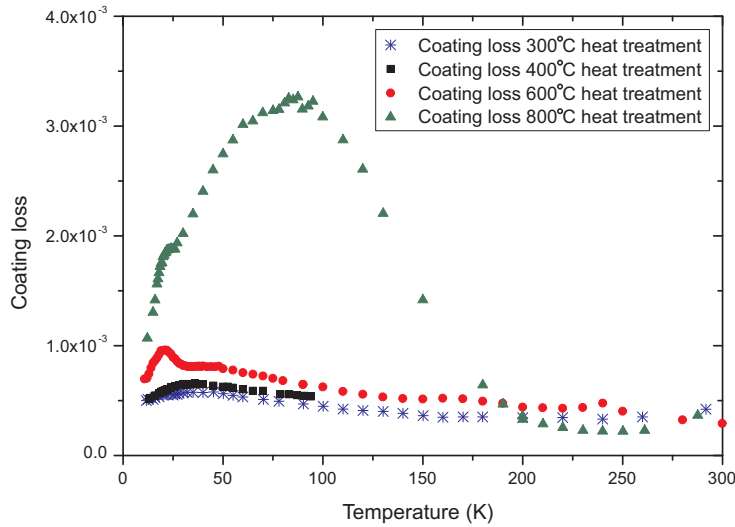


Figure 5. The calculated mechanical loss factors of the various Ta_2O_5 coatings at approximately 1900 Hz

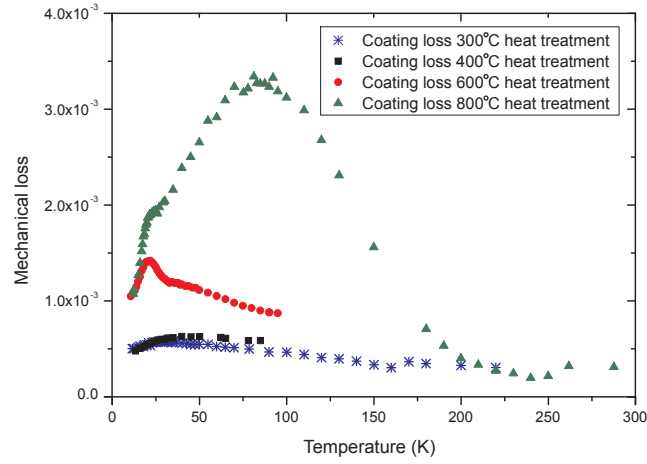


Figure 6. The calculated mechanical loss factors of the various Ta_2O_5 coatings at approximately 3000 Hz

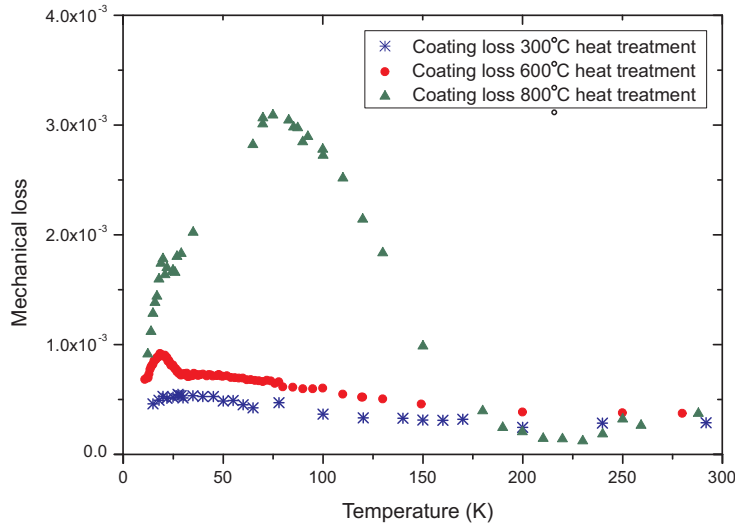


Figure 7. The calculated mechanical loss factors of the various Ta_2O_5 coatings at approximately 350 Hz

The results clearly show that the temperature of the post-deposition heat treatment had a significant effect on the temperature dependence of the mechanical loss factor of the Ta_2O_5 coatings. There are several notable features in the data. Firstly, a broad peak in the dissipation of the Ta_2O_5 film heat treated at 300 °C was observed at approximately 35 K. The data for the coated cantilever which was heat treated at 400 °C is incomplete as the cantilever cracked in the clamp during a measurement cycle. The breakage was indicated by a sudden change in the resonant frequencies of the cantilever and an increase in the measured mechanical dissipation factors. However, below 100 K the loss of this coating follows a similar trend to the coating heat treated at 300 °C, with a broad dissipation peak at 35 K.

Secondly, a sharper additional peak in the dissipation of the Ta_2O_5 film heat treated at $600^\circ C$ was observed at approximately 20 K. This is in qualitative agreement with previous measurements of Ta_2O_5 films supplied by LMA[†] and heat treated at the same temperature [22, 26]. This peak at 20 K is significantly narrower and higher than the peak at 35 K observed in the coatings heat treated at 300 and $400^\circ C$. At temperatures above 40 K, the dissipation of the coating heat treated at $600^\circ C$ shows a similar trend in shape to that for the 300 and $400^\circ C$ coatings, although the absolute level of dissipation is somewhat higher below 250 K. This suggests that the 35 K peak may also be present in the film heat-treated at $600^\circ C$, partially underlying the tail of the 20 K peak.

Thirdly, the Ta_2O_5 coating treated at $800^\circ C$ exhibits a large and very broad dissipation peak at 80 to 90 K. A small plateau in the low temperature edge of this peak is apparent at each measurement frequency, suggesting that the 20 K dissipation peak is also present. At temperatures between 200 and 250 K, this coating has a lower dissipation than those heat treated at lower temperatures, with the minimum dissipation occurring at approximately 225 K. The increase in the dissipation between 225 K and 300 K may be indicative of an additional dissipation peak occurring above room temperature. However, further investigation was beyond the scope of the current study, as the sensitivity with which the loss factor of the coating can be measured is significantly reduced at room temperature and above due to the relatively high dissipation factor of the silicon cantilever substrates at these temperatures.

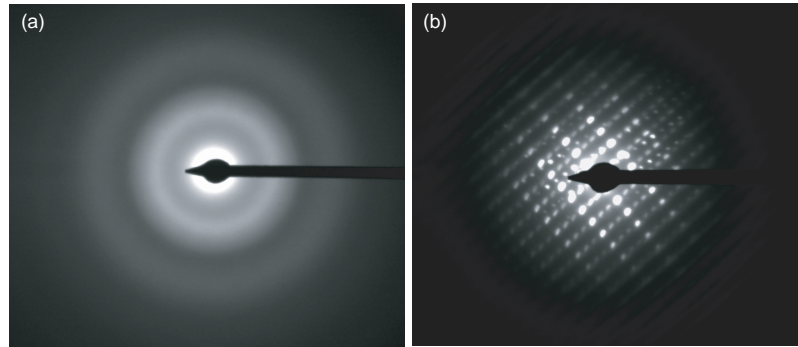


Figure 8. (a) Electron diffraction pattern from the Ta_2O_5 coating heat treated at $600^\circ C$. The diffuse rings indicate an amorphous structure. (b) Electron diffraction pattern from the Ta_2O_5 coating heat treated at $800^\circ C$, indicating crystalline structure.

As noted above, ion-beam sputtered Ta_2O_5 has been observed to crystallize at temperatures between 600 and $700^\circ C$. The structure of the Ta_2O_5 films was investigated by electron diffraction measurements of the witness samples which were coated and heat treated at the same time as the cantilevers. The results, shown in Figure 8, indicate that the coatings heat treated at $600^\circ C$ and below are amorphous, while the coating heat treated at $800^\circ C$ has a crystalline structure. The difference in structure is also apparent from comparison of transmission electron microscope (TEM) images of the

[†] Laboratoire des Matériaux Avancés, LMA, CNRS-IN2P3, France, <http://lma.in2p3.fr>.

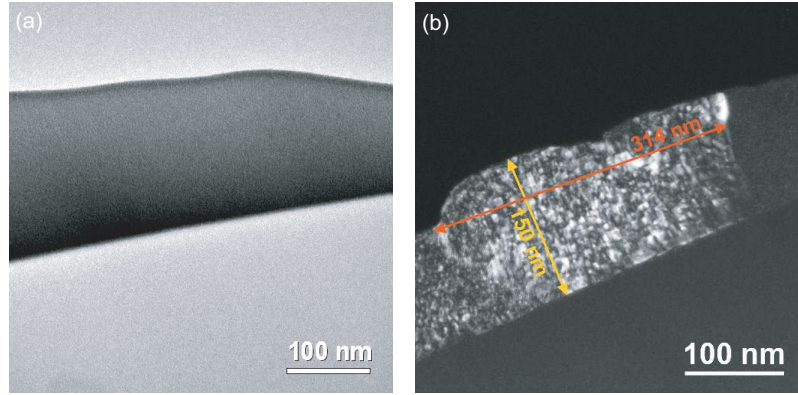


Figure 9. (a) Bright field TEM image of a typical amorphous Ta_2O_5 film (darker region), heat treated at 600 °C. (b) Dark field TEM image of a crystallized Ta_2O_5 film (lighter region) which was heat treated at 800 °C.

coatings heat treated at 600 and 800 °C, as shown in Figure 9. It is likely therefore that the large dissipation peak centered on 80 to 90 K is associated with the poly-crystalline structure of the Ta_2O_5 induced by the heat treatment at 800 °C. One possible dissipation mechanism in poly-crystalline materials is phonon scattering at the grain boundaries [44].

4. Analysis

For both the dissipation peak near 20 K and the peak near 35 K, the temperature at which the peak occurred was found to vary with frequency. This behaviour, which can be seen clearly in Figure 10 for the coating heat treated at 600 °C, is a typical characteristic of a thermally activated dissipation process. These processes can be characterized by a rate constant, τ_0 , and an activation energy, E_a , which are related by the Arrhenius equation [44]:

$$\tau = \tau_0 e^{E_a/k_B T} \quad (4)$$

where τ is the relaxation time associated with the dissipative system returning to equilibrium after a perturbation. Analysis of these dissipation processes shows that the temperature of the dissipation peak, T_{peak} , at angular frequency ω_0 is related to the activation energy and rate constant as follows [44]:

$$\omega_0 \tau_0 e^{E_a/k_B T_{\text{peak}}} = 1. \quad (5)$$

Thus a plot of $\log \omega_0$ against $1/T_{\text{peak}}$ should yield a straight line, from which the activation energy and rate constant for the dissipation process can be obtained. Figure 11 shows this analysis for the peak near 20 K in the coating heat treated at 600 °C. The activation energy and rate constant, calculated from the linear fit, were found to be (35.6 ± 2.5) meV and $(9.9 \pm 0.5) \times 10^{-13}$ s respectively. The activation energy is somewhat higher than a previous measurement of (28.6 ± 1.6) meV for Ta_2O_5 deposited by LMA. The difference in activation energy could arise from differences in the detailed structure

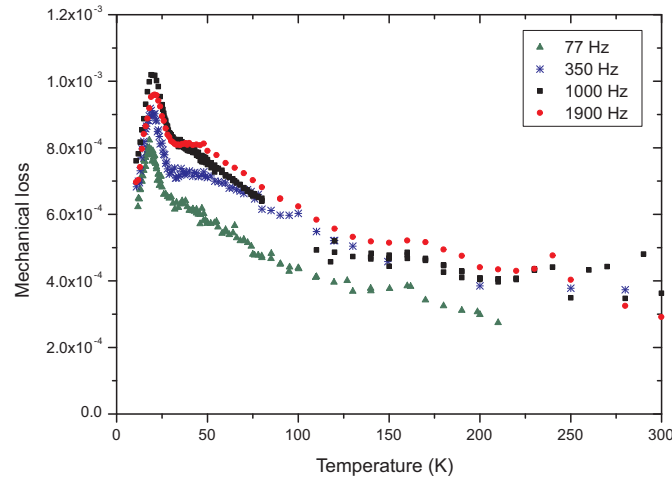


Figure 10. Mechanical dissipation of the coating heat treated at $600\text{ }^{\circ}\text{C}$ at several frequencies, showing the frequency dependence of the temperature of the peak in the low temperature dissipation.

of the amorphous coating induced by variations in the ion-beam sputtering deposition process between coating vendors.

The Arrhenius plot for the peak near 35 K observed for the coating heat treated at $300\text{ }^{\circ}\text{C}$ is shown in Figure 12. A straight line could be fitted to the data for four of the modes studied. However, the point on the Arrhenius plot corresponding to the mode at 3200 Hz clearly does not follow this linear trend. It is possible that a torsional mode close in frequency to the 5th bending mode was measured unintentionally, which may explain the difference in the loss peak for this mode. If this point is neglected the fit for the remaining modes gives an activation energy of $(66 \pm 10)\text{ meV}$ and a rate constant of $(9.4 \pm 0.9) \times 10^{-14}\text{ s}$.

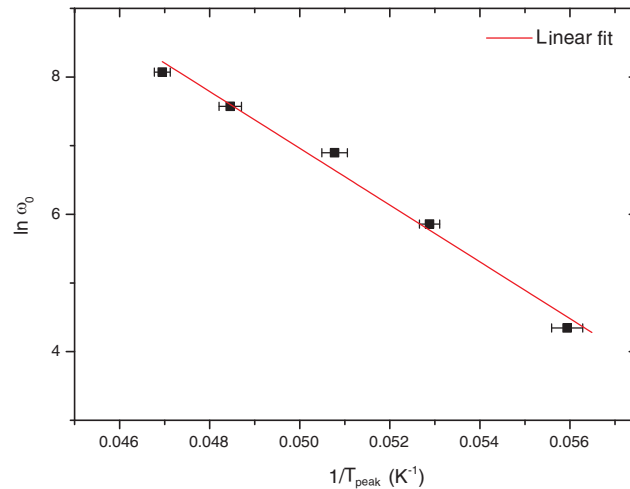


Figure 11. Arrhenius plot for loss peak at 20 K observed in the Ta_2O_5 coating heat treated at $600\text{ }^{\circ}\text{C}$

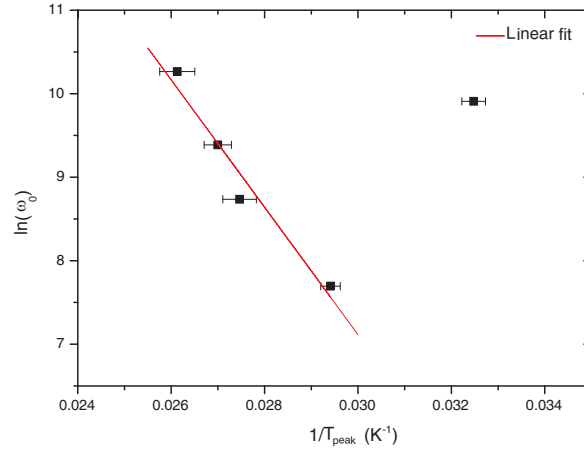


Figure 12. Arrhenius plot for loss peak at 35 K observed in the Ta_2O_5 coating heat treated at 300 °C

In many amorphous solids, the dissipation at temperatures above 10 K is thought to result from thermally activated reorientations of bonds over potential barriers of height V [45]. If the dissipation is modelled as arising from transitions in an asymmetric double-well potential in some local configuration coordinate, it can be shown that the measured mechanical loss is related to the distribution of energy barrier heights $g(V)$ by the following expression [46]:

$$\phi = \frac{\pi\gamma^2 f_0}{C_{ii}} k_B T g(V), \quad (6)$$

where

$$V = k_B T \ln\left(\frac{1}{\omega\tau_0}\right). \quad (7)$$

and C_{ii} is the appropriate elastic constant for the mode-shape under consideration, γ is the elastic coupling constant which represents the coupling between the defect (e.g. a bond re-orienting within the double well potential) and the applied strain and f_0 is a constant representing the asymmetry between the depth of the two potential wells in each double-well system. The relaxation time τ associated with a barrier height V is given by Equation 4. The assumptions made in this model are discussed in detail by Topp and Cahill [46].

Thus the measured mechanical loss can be used to extract the distribution of barrier heights (i.e. activation energies) for the loss mechanism associated with a particular dissipation peak. The extracted barrier height distributions for the Ta_2O_5 heat treated at 300 °C and 600 °C are shown in Figure 13. At all barrier energies, the magnitude of the function $g(V)f_0$ is larger for the coating heat treated at 600 °C. An interpretation of this is that there are more barriers contributing to the dissipation in this coating, resulting in a higher mechanical dissipation. The feature in the distribution function at a barrier height energy of 35 meV corresponds to the average activation energy calculated from the Arrhenius plot. This feature appears to be superimposed on a background distribution similar to that found for the coating heat treated at 300 °C.

The shape of the barrier height distribution for the 35 K loss peak in the coating heat treated at 300 °C is broadly similar to the distribution found in bulk fused silica [46], with $g(V)f_0$ decreasing smoothly with increasing barrier energy. We postulate that the dissipation mechanisms in Ta_2O_5 may be similar to that in fused silica and other amorphous solids, and be related to the reorientation of oxygen atoms, or groups of tantalum and oxygen atoms, in a double-well potential. Several models of the dissipation mechanism in fused silica have been proposed, including motion of Si-O bonds between stable angles [47], elongation of Si-O bonds [25], rotation of SiO_4 tetrahedral structures [48, 49] or of groups of these structures [50]. If similar processes are responsible for the loss in Ta_2O_5 , it is possible that the peaks observed at 20 K and 35 K correspond to two different types of motion, one of which is only activated by changes in the local ordering induced by heat treatment at temperatures close to the crystallization temperature. Further detailed studies of the short range structure in Ta_2O_5 coatings using electron diffraction data and computer modelling are ongoing [51].

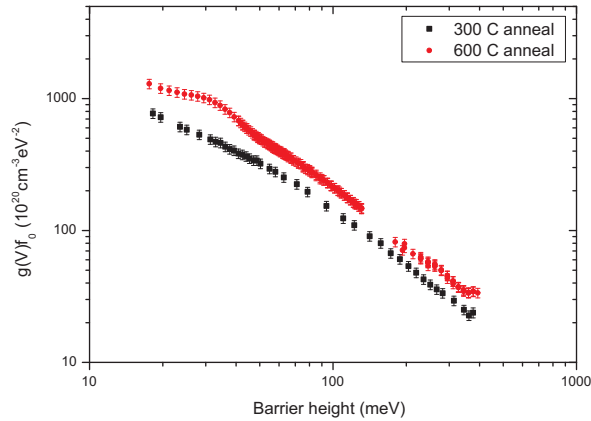


Figure 13. Comparison of the calculated potential barrier height distribution function $g(V)f_0$ as a function of barrier height for Ta_2O_5 heat treated at 300 °C and 600 °C, using the data measured at ~ 1000 Hz.

5. Conclusions

The temperature dependence of the mechanical dissipation in Ta_2O_5 films has been found to be strongly dependent on the temperature at which post-deposition heat treatment is carried out. We have identified three dissipation peaks arising from dissipation mechanisms which occur after heat treatment at different temperatures. The previously observed dissipation peak at 20 K has been shown to arise from heat treatment close to the temperature at which the amorphous Ta_2O_5 crystallizes. The dissipation mechanism responsible for this peak may therefore be related to pre-crystallization changes in the local ordering of the Ta_2O_5 film. A dissipation peak at approximately 35 K was observed in Ta_2O_5 films heat-treated at 300 and 400 °C. There is evidence

that this peak is also present in Ta₂O₅ heat treated at 600 °C, underlying the larger dissipation peak at 20 K. We postulate that the two low temperature dissipation peaks may arise from two different types of thermally activated transitions. The Ta₂O₅ film heat-treated at 800 °C, which was found to have crystallized, had a very broad dissipation peak centered on 90 - 100 K.

Below 200 K the dissipation of the Ta₂O₅ coatings was found to increase at higher heat treatment temperatures, suggesting that minimizing the temperature at which post-deposition heat treatment is carried out may allow a significant decrease in the coating thermal noise in future cryogenic gravitational wave detectors, thus extending their astronomical reach. As heat treatment is also known to affect the optical absorption of dielectric coating, studies of the optical properties of Ta₂O₅ heat-treated at various temperatures would be of interest.

The dissipation of Ta₂O₅ coatings at room temperature appears to be related to the broad tail of the dissipation peak at 35 K. However there is some evidence, particularly for the coating heat-treated at 800 °C, of an increase in dissipation close to room temperature. Thus further study of the dissipation in Ta₂O₅ at temperatures above 300 K would be of significant interest to determine if additional dissipation peaks occurring at temperatures greater than 300 K may contribute to the room temperature dissipation.

Further work is underway to investigate the relationship between the short range structure of Ta₂O₅ films and the mechanical loss. In addition, it would be of significant interest to study the emergence of the various dissipation peaks in Ta₂O₅ by studying coatings heat treated at more temperature intervals between 400 and 800 °C.

Acknowledgments

We are grateful for the financial support provided by STFC, the University of Glasgow, EPSRC, the German Science Foundation under contract SFB Transregio 7 and the National Science Foundation under grants PHY-07 57896 and PHY-05 02641 (Stanford) and NSF-0653590 (HWS). I. Martin and S. Reid are supported by an STFC Postdoctoral Fellowship and a Royal Society of Edinburgh Research Fellowship respectively. R. Nawrodt acknowledges the support of the FP7 EU Einstein Telescope design study project under contract number 211743. LIGO was constructed by the California Institute of Technology and Massachusetts Institute of Technology with funding from the National Science Foundation and operates under cooperative agreement PHY-0107417. We would like to thank our colleagues in the LSC and VIRGO collaborations and within SUPA for their interest in this work. This paper has LIGO Document Number LIGO-P1000074.

- [1] A. Abramovici, W. E. Althouse, R. W. P. Drever, Y. Gursel, et al., *Science* **256** (1992) 325–333.
- [2] H. Lück, M. Hewitson, P. Ajith, B. Allen, et al., *Class. Quantum Grav.* **23** (2006) S71–S78.
- [3] F. Acernese, P. Amico, M. Alshourbagy, F. Antonucci, et al., *Class. Quantum Grav.* **24** (2007) S381–S388.
- [4] R. Takahashi, the TAMA Collaboration, *Class. Quantum Grav.* **21** (2004) S403–S408.
- [5] P. Saulson, *Phys. Rev. D* **42** (1990) 2437–2445.
- [6] H. B. Callen, R. F. Greene, *Phys. Rev.* **86** (1952) 702–710.

- [7] H. B. Callen, T. A. Welton, Phys. Rev. **83** (1951) 34–40.
- [8] G. M. Harry, for the LIGO Scientific Collaboration, Class. Quantum Grav. **27** (2010) 084006.
- [9] R. Flaminio, A. Freise, A. Gennai, P. Hello, Advanced Virgo White Paper, Virgo internal document VIR-NOT-1390-304 (2005).
URL <http://wwwcascina.virgo.infn.it/advirgo/docs/whitepaper.pdf>
- [10] Y. Levin, Phys. Rev. D **57** (1998) 659–663.
- [11] N. Nakagawa, A. M. Gretarsson, E. K. Gustafson, M. M. Fejer, Phys. Rev. D **65** (2002) 102001.
- [12] G. Harry, A. Gretarsson, P. Saulson, S. Kittelberger, et al., Class. Quantum Grav. **19** (2002) 897–917.
- [13] D. R. M. Crooks, P. Sneddon, G. Cagnoli, J. Hough, et al., Class. Quantum Grav. **19** (2002) 883–896.
- [14] R. J. Rafac, B. C. Young, J. A. Beall, W. M. Itano, et al., Phys. Rev. Lett. **85** (2000) 2462–2465.
- [15] A. D. Ludlow, M. M. Boyd, T. Zelevinsky, S. M. Foreman, et al., Phys. Rev. Lett. **96** (2006) 033003.
- [16] S. A. Webster, M. Oxborrow, P. Gill, Opt. Lett. **29** (2004) 1497–1499.
- [17] F. Schmidt-Kaler, S. Gulde, M. Riebe, T. Deuschl, et al., Journal of Physics B: Atomic, Molecular and Optical Physics **36** (2003) 623–636.
- [18] S. D. Penn, P. H. Sneddon, H. Armandula, J. C. Betzwieser, et al., Class. Quantum Grav. **20** (2003) 2917–2928.
- [19] D. Crooks, G. Cagnoli, M. Fejer, A. Gretarsson, et al., Class. Quantum Grav. **21** (2004) 1059–1065.
- [20] D. R. M. Crooks, G. Cagnoli, M. M. Fejer, G. Harry, et al., Class. Quantum Grav. **23** (2006) 4953–4965.
- [21] G. M. Harry, M. R. Abernathy, A. E. Becerra-Toledo, H. Armandula, et al., Class. Quantum Grav. **24** (2007) 405–415.
- [22] I. Martin, H. Armandula, C. Comtet, M. M. Fejer, et al., Class. Quantum Grav. **25** (5) (2008) 055005.
- [23] V. B. Braginsky, V. P. Mitrofanov, V. I. Panov, *Systems with small dissipation*, University of Chicago Press, Chicago, 1985.
- [24] H. E. Bömmel, W. P. Mason, A. W. Warner, Phys. Rev. **102** (1956) 64–71.
- [25] R. E. Strakna, Phys. Rev. **123** (1961) 2020–2026.
- [26] I. Martin, H. Armandula, C. Comtet, M. M. Fejer, et al., Class. Quantum Grav. **26** (2009) 155012.
- [27] R. P. Netterfield, M. Gross, F. N. Baynes, K. L. Green, et al., Proc. SPIE **5870** (2005) 58700H.
- [28] M. Tilsch, V. Scheuer, T. T. Tschudi, Proc. SPIE **3133** (1997) 163–175.
- [29] J. T. Brown, Appl. Opt. **43** (2004) 4506–4511.
- [30] A. J. Waldorf, J. A. Dobrowolski, B. T. Sullivan, L. M. Plante, Appl. Opt. **32** (1993) 5583–5593.
- [31] K. Numata, K. Yamamoto, H. Ishimoto, S. Otsuka, et al., Phys. Lett. A **327** (2004) 263–271.
- [32] B. S. Lunin, *Physical and Chemical Bases for the Development of Hemispherical Resonators for Solid-State Gyroscopes*, Moscow Aviation Institute, Moscow, 2005.
- [33] M. Punturo, et al., Einstein Gravitational Wave Telescope, proposal to the European Commission, Framework Programme 7, <http://www.ego-gw.it/ILIAS-GW/FP7-DS/fp7-DS.htm>.
- [34] K. Kuroda, et al., Status of LCGT, Class. Quantum Grav. **27** (2010) 084004.
- [35] T. J. Quinn, C. C. Speake, R. S. Davis, W. Tew, Phys. Lett. A **197** (1995) 197–208.
- [36] K. Y. Yasamura, T. D. Stowe, E. M. Chow, T. Pfafman, et al., J. Microelectromech. Sys. **9** (2000) 117–125.
- [37] R. Netterfield, CSIRO Report, Ion Beam Deposited Coatings, LIGO Document Control Centre No. T040236-00-D (2004).
URL <http://www.ligo.caltech.edu/docs/T/T040236-00/>
- [38] N. W. McLachlan, *Theory of Vibrations*, Dover, 1952.
- [39] B. E. White, R. O. Pohl, Phys. Rev. Lett. **75** (1995) 4437–4439.
- [40] B. S. Berry, W. C. Pritchett, IBM J. Res. Dev. **19** (1975) 334–343.
- [41] Y. S. Touloukian, E. H. Buyco, *Thermo-physical Properties of Matter*, Plenum, New York, 1970.

- [42] P. Martin, et al., in: P. Townsend, T. Weihs, J. Sanchez, P. Borgesen (Eds.), Materials Research Society Symposium Proceedings, Vol. **308**, Materials Research Society, 1993, pp. 583–588.
- [43] J. W. Marx, J. M. Sivertsen, Journal of Applied Physics **24** (1952) 81–87.
- [44] A. Nowick, B. Berry, *Anelastic Relaxation in Crystalline Solids*, Academic Press, New York, 1972.
- [45] K. S. Gilroy, W. A. Phillips, Philos. Mag. B **43** (1981) 735–746.
- [46] K. A. Topp, D. G. Cahill, Z. Phys. B: Condens. Matter **101** (1996) 235–245.
- [47] O. L. Anderson, H. E. Bommel, J. Am. Ceram. Soc. **38** (1955) 125–131.
- [48] M. R. Vukceovich, J. Non-Cryst. Solids **11** (1972) 25–63.
- [49] U. Buchenau, N. Nücker, A. J. Dianoux, Phys. Rev. Lett. **53** (1984) 2316–2319.
- [50] J. Reinisch, A. Heuer, Phys. Rev. Lett. 95 (2005) 155502.
- [51] R. Bassiri, K. B. Borisenko, D. J. H. Cockayne, J. Hough, et al., J. Phys. Conf. Ser. in press.